ELSEVIER

Catalysis Today 20 (1994) 351–366

catalysis today

Enhancement of catalytic reaction by pressure swing adsorption

D. Chatsiriwech[a], E. Alpay[a], L.S. Kershenbaum[a,*], C.P. Hull[b], N.F. Kirkby[b]

[a]*Department of Chemical Engineering and Chemical Technology, and the Centre for Process Systems Engineering, Imperial College of Science, Technology and Medicine, Prince Consort Road, London, SW7 2BY, United Kingdom*

[b]*Department of Chemical and Process Engineering, University of Surrey, Guildford, Surrey, GU2 5XH, United Kingdom*

Abstract

A theoretical study of an adsorptive reactor which combines multibed pressure swing adsorption and chemical reaction is presented; such a reactor is referred to as a pressure swing reactor, or PSR. Studies have concentrated on an asymptotic case in which there is the ideal propagation of concentration waves within the reactor beds; the method of characteristics was employed in the solution of the governing PSR equations. The studies assessed the effects of operating conditions, and cycle configurations, on the PSR performance. Calculations indicate enhanced reactant conversion when compared to conventional steady state plug flow operation. In particular, for some reversible reactions, substantial improvements over equilibrium yields have been calculated. For example, for the dissociation reaction $2A \Leftrightarrow B + C$, and where B is the only adsorbing component, approximately two-fold improvements over the equilibrium yield of product B have been predicted. Such reaction enhancement can be attributed to the limitation of the backward reaction, which results from the separation of the product species B and C.

In addition to the method of characteristics, a cells-in-series method for the asymptotic case has been developed, and found to yield calculations consistent with the method of characteristics solutions. In a third numerical approach, the spatial discretisation technique of orthogonal collocation on finite elements was applied to the governing PSR equations, and the resulting system of ordinary differential equations solved by a standard integration algorithm. In this case, many of the simplifying model assumptions were relaxed, allowing, for example, the simulation of a non-isothermal PSR with finite mass transfer rates.

One practical significance of reaction enhancement by pressure swing adsorption is a lower temperature of operation than in a conventional reactor. This would lead to savings in the energy requirements of the reactor, and limit the rate and degree of catalyst deactivation due to coke deposition or sintering.

*Corresponding author.

SSDI 0920-5861(94)00049-8

1. Introduction

Adsorptive reactors couple the operations of separation and chemical reaction into a single process. One of the first examples of such a process is the chromatographic reactor (see, for example, refs. [1–3] and extensions of which include real and simulated moving bed processes (see refs. [4–6]). Such reactors have advantages over conventional steady flow reactors in that enhanced reactant conversion can be achieved. Consider, for example, a reactant A flowing through a packed bed, and undergoing a reversible elementary dissociation reaction $2A \Leftrightarrow B + C$. The reversible adsorption of a product component, say B, results in the separation of B and C in both axial space, and across the solid and gas phases. Subsequently, reaction in the backward direction is constrained, shifting the reaction equilibrium towards the further production of B and C. In the case of industrially important endothermic reactions (e.g. cracking, dehydrogenation, hydrogenolysis), equilibrium limitations often dictate the necessity of high temperature operation to achieve realistic levels of conversion. Reaction enhancement could allow a lower temperature of operation for a given conversion, thus giving savings on the process energy requirements. It could also make a catalytic process feasible since a lower temperature of operation would reduce the degree of catalyst deactivation due to, for example, coke deposition or sintering. However, major disadvantages of the chromatographic type reactors include non-continuous and relatively complex operation, especially in the case of the moving bed processes. Similiarly, the use of membrane reactors for achieving simultaneous reaction and separation has many problems to overcome before its obvious potential can be realised. The scope for research for novel adsorptive reactors is therefore apparent.

This paper presents a theoretical study of an adsorptive reactor which combines multibed pressure swing adsorption (PSA) and chemical reaction. A schematic diagram of such a reactor, which is referred to as a pressure swing reactor (or PSR), is given in Fig. 1. Typically, the reactor would be packed with a mixture of an active catalyst for the reaction, and a selective adsorbent for the adsorption of one or more of the reaction species. Conventional steps for separation by pressure swing adsorption are employed; see refs. [7,8]. The three steps of pressurisation, product release and depressurisation constitute the simple cycle. In order to achieve a continuous flow of exit gases, two beds are coupled and operated in the sequence indicated in Fig. 1. Other steps can be incorporated into the simple cycle so as to enhance product recovery or bed regeneration. For the latter, one such step is the countercurrent purge step, and has been considered in this work. A schematic diagram of the purge step, and sequencing for a two bed purge cycle, are also shown in Fig. 1. Important advantages of the PSR include a relatively simple operation, based on extensions of an existing industrial process and established mechanical technology, and the continuous delivery of product. A PSR may therefore be suitable for large scale applications.

In the following sections, models for a PSR are presented, and calculations illustrating the potential of the process given. Emphasis is given to the reversible dissociation type reactions, and in particular to $2A \Leftrightarrow B + C$. Possible practical examples of dissociation reactions include the dehydrogenation reactions of ethane to ethylene, and propane to propylene. As noted above, conventional reactors for these are usually operated at high

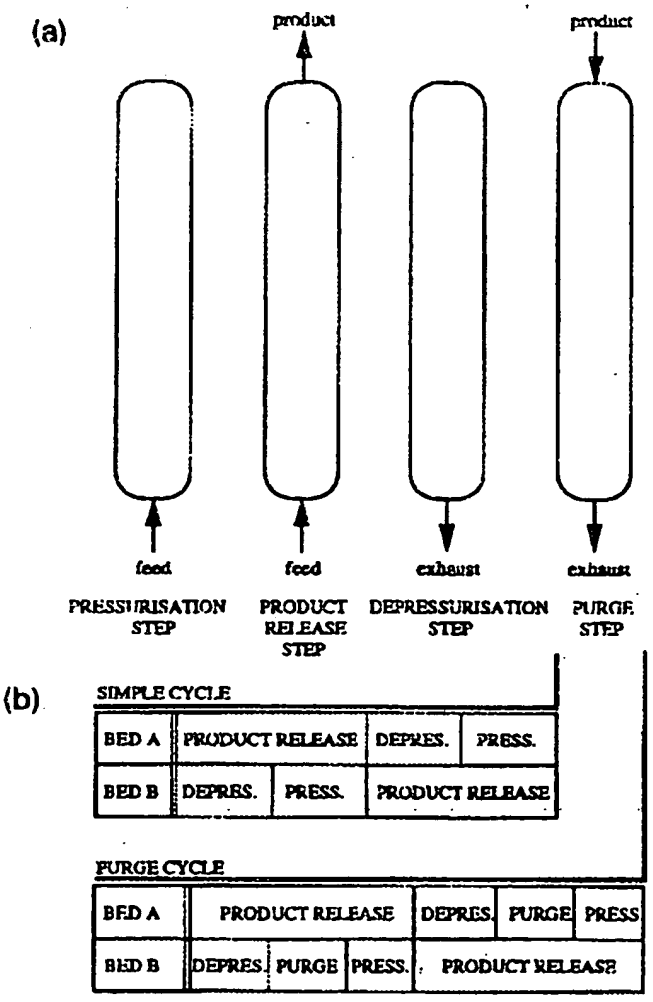

Fig. 1. Schematic diagram of a PSR showing the basic steps of operation. (b) Sequencing of the steps for two-bed processes employing simple and purge cycles.

temperatures so as to overcome kinetic and, especially, thermodynamic constraints, albeit at the expense of high energy requirements. Catalytic processes for these reactions are not generally feasible because of the rapid catalyst deactivation due to coking which would occur at these temperatures. It is important to note that unlike the test case reaction scheme chosen for this study, the case of a real dehydrogenation is complicated by the effects of the pressure dependence of the equilibrium yield. The equilibrium conversion of $2A \Leftrightarrow B + C$ is pressure independent, and thus provides a simplified test case for the analysis of pressure swing reaction. However, where there is a net increase in moles due to reaction, a low pressure (or low average pressure) will be desirable for high reaction conversion, even though a large pressure ratio is generally desirable for the maximum separation effect.

2. Theoretical

Difficulties in the simulation of PSR arise from the non-linear nature of the system, and the inherent solution discontinuities or steep gradients in concentrations. A further complexity arises from the step-wise (or ramp-wise) changes in pressure at the feed end of the bed, causing periodic reversals in the gas flow direction within the bed. In this work, three numerical approaches to the problem have been adopted: the method of characteristics (MOC), and spatial discretisation methods based on cells-in-series (CIS) and orthogonal collocation on finite elements (OCFE). The first two approaches were applied to a simple model in which, for example, pressure gradients along the length of the bed were neglected, reaction species assumed dilute, and linear adsorption isotherms employed. These conditions result in a situation in which there is the ideal propagation of a concentration wave fronts, i.e., no dispersive effects on the wave fronts. CIS discretisation was carried out using the General Process Modelling System (gPROMS) of Barton and Pantelides [9], currently under continued development at Imperial College. OCFE discretisation provided a means for the simulation of models which relax many of the usual assumptions employed in describing pressure swing processes. Further details of these numerical approaches are now given.

2.1. *Method of characteristics*

Principal assumptions for the simple case model are as follows. (1) Plug flow of gases. (2) Dilute reactants in an inert and non-adsorbing carrier. (3) An isothermal process. (4) No axial pressure gradients. (5) No radial pressure or concentration gradients. (6) Instantaneous local equilibrium between the bulk gas and adsorbed phases. (7) Linear adsorption isotherms. (8) Simple power-law reaction kinetics. (9) Beds consisting of a uniform mixture of catalyst and adsorbent particles. Given these assumptions, and for the dissociation reaction $2A \Leftrightarrow B + C$, total and component material balances for a PSR bed can be written as

$$\frac{\partial u}{\partial z} + P' = 0 \tag{1}$$

and

$$u\frac{\partial y_i}{\partial z} + \beta_i\frac{\partial y_i}{\partial t} + (\beta_i - 1)P'y_i - \nu_i\left(\frac{1-\varepsilon}{\varepsilon}\right)\left(\frac{\rho RT}{P}\right)r_x = 0 \tag{2}$$

respectively, where

$$P' = \frac{1}{P}\frac{dP}{dt} \tag{3}$$

$$\beta_i = 1 + \left(\frac{1-\varepsilon}{\varepsilon}\right)\rho RTm_i \tag{4}$$

$$r_x = k_f(C_A^2 - C_B C_C/K_C) \tag{5}$$

$$\nu_A = 2,\ \nu_{B,C} = -1 \tag{6}$$

and where ε is the total voidage, ρ is the solid density (kg m^{-3}), C is the gas phase concentration (mol m^{-3}), k_f is the forward reaction rate constant (m^6 kg^{-1} mol^{-1} s^{-1}), K_C is the reaction equilibrium constant, m is the adsorption isotherm gradient (mol kg^{-1} Pa^{-1}), P is pressure (Pa), r_x is the reaction rate (mol kg^{-1} s^{-1}), R is the gas constant, t is time (s), T is temperature (K), u is the superficial gas velocity (m s^{-1}), y is the gas phase mole fraction, z is the axial space coordinate (m), and the subscript i a component identifier. Modified formulations of Eqs. (4) and (5) yield models for other reaction schemes.

Boundary conditions during the four steps of operation considered in this work are given in Table 1. These define the rate of pressurisation or depressurisation (dP/dt), the exit velocity of the carrier gas, u_L, and the mole fractions of reactant species at $z=0$ or $z=L$.

The analytical solution of Eq. (1) can be readily written as

$$u = u_L + P'(L-z) \tag{7}$$

The component balances are of a hyperbolic form, and can therefore be solved by the method of characteristics; see, for example, Holland and Liapis [10], and more specifically Morgan and Kirkby [11]. Application of this method to Eq. (2) yields a set of characteristics which describe the characteristic directions, i.e.,

$$\frac{dz}{dt} = \frac{u}{\beta_i} = \frac{u_L + P'(L-z)}{\beta_i} \tag{8}$$

and the variation of gas composition with time along these, i.e.,

$$\frac{Dy_i}{Dt} = \frac{1}{\beta_i}\left[(1-\beta_i)P'y_i + \nu_i\left(\frac{1-\varepsilon}{\varepsilon}\right)\left(\frac{\rho RT}{P}\right)r_x\right] \tag{9}$$

Eqs. (8) and (9) are suitable for integration by a standard integration algorithm. It is important to note however, that since the reaction term is a function of the compositions of all components, then for a given set of characteristics, and say for component j, gas composition values need to be determined for all other components, $i \neq j$, at the given z and t. For each component $i \neq j$, this is achieved by interpolation in the z domain, at a given t, between adjacent characteristics. In this work, a Runge–Kutta–Merson integration algorithm was used, and linear or non-linear interpolation employed at the end of every integration time-step. At the cyclic steady state (CSS), checks on the component material balances for the MOC solutions (over a complete cycle) were found to be less than 2% in error. These indicate the good numerical accuracy of the model solution.

Table 1
Boundary and other conditions for the PSR process

Process step	dP/dt	$u_{z=L}$	y_i ($z=0$)	y_i ($z=L$)
Pressurisation	Constant > 0	0	Constant	–
Product release	0	Constant > 0	Constant	[a]
Depressurisation	Constant < 0	0	[a]	...
Purge	0	Constant < 0	[a]	[b]

[a] Determined from the material balances.
[b] Based on the average mole fraction of gas collected during the product release step.

2.2. Cells-in-series: gPROMS

In the CIS discretisation method, the bed is divided into a series of well-mixed cells. The well-mixed assumption eliminates spatial gradients within a cell, whilst a spatial gradient is maintained from one cell to the next. The governing partial differential equations of the PSR model are discretised for each cell, and the resulting system of ordinary differential equations solved by a standard integration algorithm. Solution accuracy (or convergence) generally increases with the number of cells, as does the plug flow condition.

For cyclic gas flow in a packed bed, a further consideration is required when using CIS, i.e., a particular cell can be in one of four general states at any instant in time. The four cell states represent the direction of pressurisation or depressurisation from each end of a cell; material balances for these will vary accordingly. For no axial pressure gradients, as in the model described in Section 2.1, gas flow throughout the length of the bed, at any instant in time, can only be in one direction. Specifically, the pressurisation and product release steps are associated with gas flow from the feed to product ends of the bed (say the forward direction), and the countercurrent depressurisation and purge steps with gas flow from the product to feed ends of the bed (say the backward direction). For a given cell c of length L_c, the total material balance for the cell (based on the assumptions listed in Section 2.1) can then be written as

$$[\pm(u_{c-1}-u_c)/L_c]-P'=0 \tag{10}$$

for gas flow in the forward/backward directions. Similarly, the component material balances are given by

$$\frac{dy_{i,c}}{dt}=\frac{1}{\beta_i}\left[s+\nu_i\left(\frac{1-\varepsilon}{\varepsilon}\right)\left(\frac{\rho RT}{P}\right)r_s\right]-P'y_{i,c} \tag{11}$$

where for gas flow in the forward direction

$$s=(u_{c-1}y_{i,c-1}-u_cy_{i,c})/L_c \tag{12}$$

and for the backward direction

$$s=(-u_{c-1}y_{i,c}+u_cy_{i,c+1})/L_c \tag{13}$$

Boundary conditions are as for those listed in Table 1.

As mentioned previously, the above ordinary differential equations (Eqs. (10) to (13)) were solved using gPROMS. This provided a concise means for declaring the model equations, upon which discrete actions (at the domain boundaries) could be imposed readily from one process step to the next. Typical CIS simulations involved 100 cells; these, for a wide range of operating conditions, were found to be consistent with the MOC solutions, i.e., CSS reaction yields within 3% agreement.

2.3. Orthogonal collocation on finite elements

In the third numerical approach, the spatial discretisation technique of OCFE was applied to the partial differential equations describing a PSR. The resulting system of ordinary

differential equations were then solved by a standard integration algorithm based on Gear's method. For this case, principal model assumptions are listed below. (1) Axially dispersed plug flow of gases. (2) Non-dilute reactants in an inert carrier. (3) A non-isothermal process. (4) Axial pressure distribution as described by Darcy's Law or the Ergun equation. (5) No radial pressure or concentration gradients. (6) Mass transfer limited adsorption as described by a linear driving force model. (7) Linear or Langmuir adsorption isotherms. (8) Simple power-law reaction kinetics. (9) Beds consisting of a uniform mixture of catalyst and adsorbent particles. Different forms of the model have also been developed so as to accommodate both finite rate and instantaneous reactions. The latter involved material balances on a mass basis, and on an equation describing the reaction equilibrium constraint; see Vaporciyan and Kadlec [12]. For both forms of the model, the inclusion of axial dispersion effects eliminated any solution discontinuities; the steep gradients were then accommodated by low-order Lagrange interpolation polynomials within a finite element grid. Typically, a discretisation based on five elements, with four internal collocation points per element, was found to be computationally precise. Furthermore, when reduced to the simple case, finite element calculations were found to be consistent with the MOC and CIS solutions.

Further discussions on the application of OCFE to pressure swing problems are given by Alpay [13,14].

3. Simulation strategy

The PSR can be treated as either a separator or reactor, and performance criteria chosen for these. For the former, the degree of component separation, or the degree of enrichment of a particular component in one stream relative to another, can be assessed. In terms of a reactor, predictions of reactant conversions or product yields are useful, as are the productivities of the catalyst; see, for example, Lu et al. [15]. Ultimately, comparisons to the performance of conventional steady state reactors are required, i.e., to the performance of plug flow and stirred tank reactors. For reversible reactions, the conversions attainable by steady state operation are limited by the reaction equilibria. For pressure dependent reaction equilibria, further care is needed when comparing PSR to steady state reactor performance. For example, for a reversible reaction in a plug flow reactor (PFR) in which there is a net increase in moles, a low operating pressure will shift the reaction equilibrium towards product formation, but will also result in a low reactant residence time; hence an optimum pressure for maximum conversion may exist. Finally, it is important to note that even for pressure independent reaction equilibria, actual reaction rates for the forward and backward reactions will be functions of pressure, and thus the rates of approach to the reaction equilibria.

In this work, calculations have concentrated on the simple case described above, and the method of characteristics employed for model solution. As mentioned previously, the reaction scheme $2A \leftrightarrow B + C$ was chosen as a test case, i.e., a dissociation reaction in which the reaction equilibrium is not a function of pressure. Adsorption of the reactant A and product C were assumed negligible, leading to the desired separations between B and C, and B and A. Base case design and operating conditions were chosen for the PSR, which

Table 2
Base case PSR design and operating conditions for the reaction $2A \rightleftharpoons B + C$.

Bed length	1.0 m	Gas flow (mol/cycle): simple/purge cycles:	
Bed diameter	0.1 m		
Solid density	3000 kg/m^3	Feed	1.689/1.871
Total voidage	0.75	Product	0.182/0.182
Temperature	473 K	Purge	0/0.182
Upper pressure	10 bar		
Lower pressure	1 bar	Adsorption isotherm gradients (mol kg^{-1} Pa^{-1}):	
Step times (s): simple/purge cycles		A	0
		B	2.5×10^{-7}
Pressurisation	6/6	C	0
Product release	12/18		
Depressurisation	6/6	Reaction parameters:	
Purge	0/6		
		k_f	0.005 m^6 kg^{-1} mol^{-1} s^{-1}
		K_C	0.01563

depict a typical small scale PSA process; see Table 2. The effect of varying an operating condition (from the base case) on the CSS performance of the unit was assessed. In particular, this performance was measured in terms of the total reaction yield of product B (Y_B), and by the separation attainable between B and C ($S_{B/C}$), and B and A ($S_{B/A}$), where

$$Y_{B|css} = \frac{\text{total amount of B (mol/cycle) collected all exit streams}}{\text{total amount of A (mol/cycle) supplied as feed}} \quad (14)$$

$$S_{i/j}|_{css} = \frac{(x_i/x_j)_{\text{product stream}}}{(x_i/x_j)_{\text{exhaust stream}}} \quad (15)$$

and where x_i and x_j are the cycle-average mole fractions of components i and j respectively. In Eq. (15), the product stream refers to the gas leaving the bed during the product delivery step, and the exhaust stream as the combined gases leaving the bed during the countercurrent depressurisation and purge steps. $S_{i/j} = 1$ indicates no separation of components i and j within the PSR, whereas $S_{i/j} > 1$ indicates the enrichment of i in the product stream, and $S_{i/j} < 1$ the enrichment of i in the exhaust stream. For the test reaction chosen in this work, and for the adsorption of B only, $S_{B/A}$ and $S_{B/C}$ are expected to be less than unity. Finally, the calculated Y_B were related to the yield attainable at the reaction equilibrium and, for the given design and average feed gas flow rate, by a conventional plug flow reactor. For the latter, an operating pressure of 10 bar was chosen (i.e., the upper operating pressure of the PSR), this resulting in the attainment of the reaction equilibrium at relatively low reactant residence times.

4. Results

In Fig. 2a, PSR, PFR and equilibrium calculations of Y_B as a function of the catalyst activity, k_f, are shown, these for the design and operating conditions listed in Table 2.

Regions in which PSR yields exceed those attainable by a PFR are indicated. Furthermore, possible improvements over the equilibrium yield are indicated, whereas of course, a PFR can only approach the equilibrium yield as k_f is increased. For the case of no adsorption of B (Fig. 2b), no improvement in the PFR (and subsequently equilibrium) yield was found.

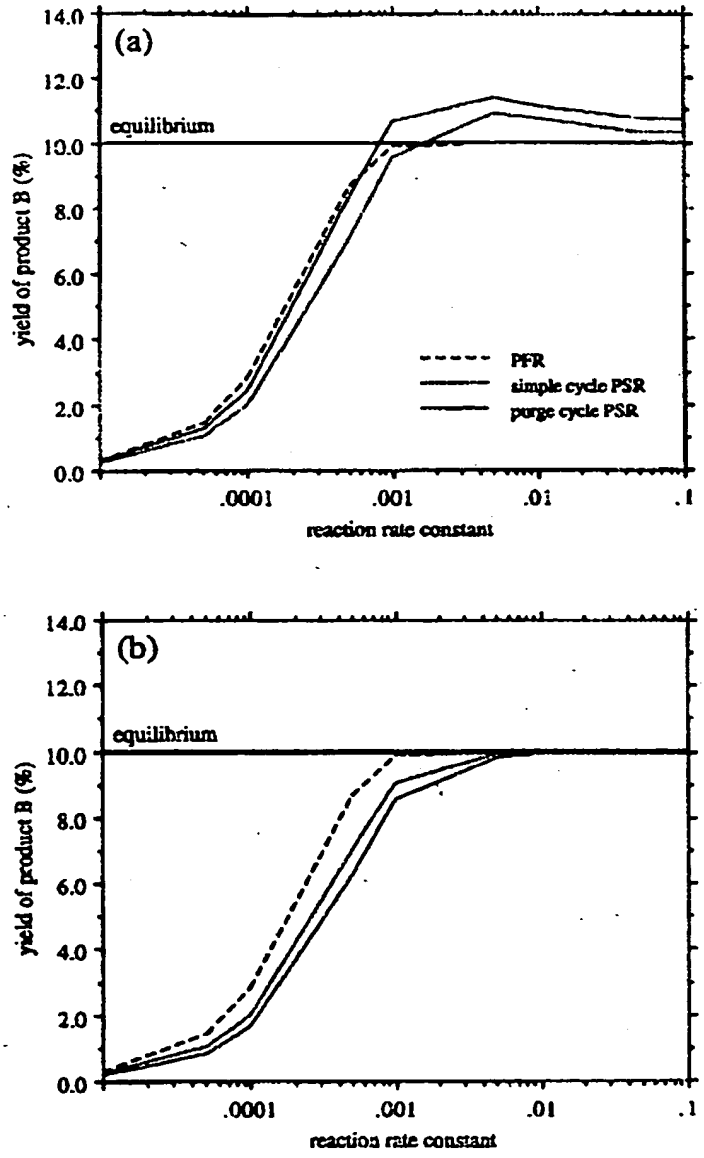

Fig. 2. Total yield of product B as a function of the forward reaction rate constant. Calculations are shown for: (a) $m_B \simeq 2.5 \times 10^{-7}$ and (b) and $m_B = 0$.

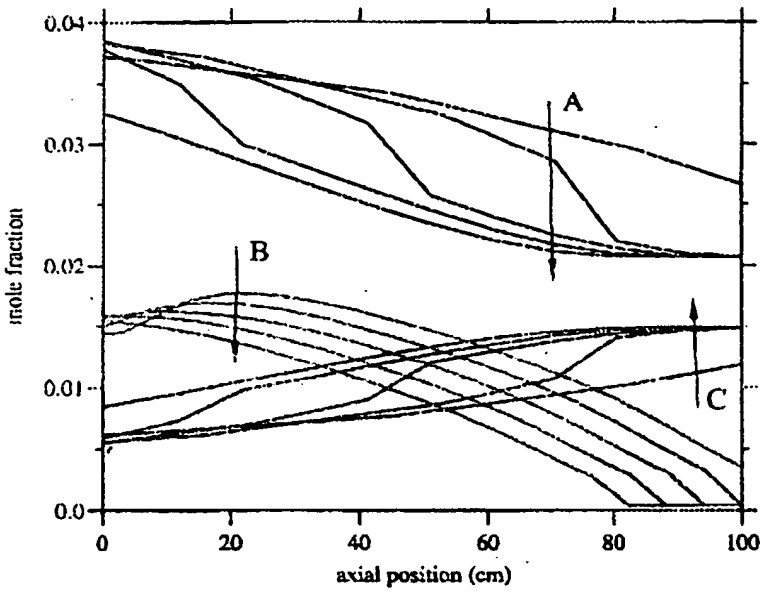

Fig. 3. Typical cyclic steady-state spatial profiles of gas composition during the purge step. Arrows indicate increasing time from the onset of the purge step.

This suggests that there is no enhancement of reaction solely due to the periodic operation of the reactor.

In terms of the mode of operation, a cycle employing a countercurrent purge step is shown to be superior to simple cycle operation; see Fig. 2a and the discussions below. As mentioned earlier, the purge step enhances bed regeneration and subsequently the separation effect. In Fig. 3 for example, typical CSS spatial profiles of gas composition during the purge step are given, these showing the concentration of product B in the purge gas exit-end of the bed (i.e., $z=0$), and the separation of the product components B and C along the length of the bed. This enhanced separation effect due to the purge step is further demonstrated by considering the simple and purge cycle configurations employed for Fig. 2a, but with a non-reacting mixture of A and B as feed. For example, for a feed mixture of 4% (v/v) A and 0.5% (v/v) B, $S_{B/A}$ for the purge and simple cycles are given as 0.000 and 0.245, respectively. Hence, greater enrichment of B in the exhaust stream (and, in fact, complete separation in this case) when employing a purge cycle.

Fig. 4a presents calculations of Y_B as a function of the important parameters of purge amount and the adsorption isotherm gradient of B, m_B. Considerable improvements over the equilibrium yields are indicated, i.e., approximately 80% improvement over the equilibrium yield. For maximum Y_B, an optimum purge amount is shown to exist. For the two sets of data shown in Fig. 4a, the higher product yields for $m_B = 2.5 \times 10^{-6}$ mol kg^{-1} Pa^{-1} correspond to the lower separation factors (thus greater effective separation between components) given in Fig. 4b. The optimum purge amount, however, does not correspond to any minimum in the separation factor–purge amount plots. For the case of no adsorption of B (calculations not shown), Y_B falls below that attainable at the reaction equilibrium and by PFR operation; $S_{B/A}$ and $S_{B/C}$ equal unity for this case.

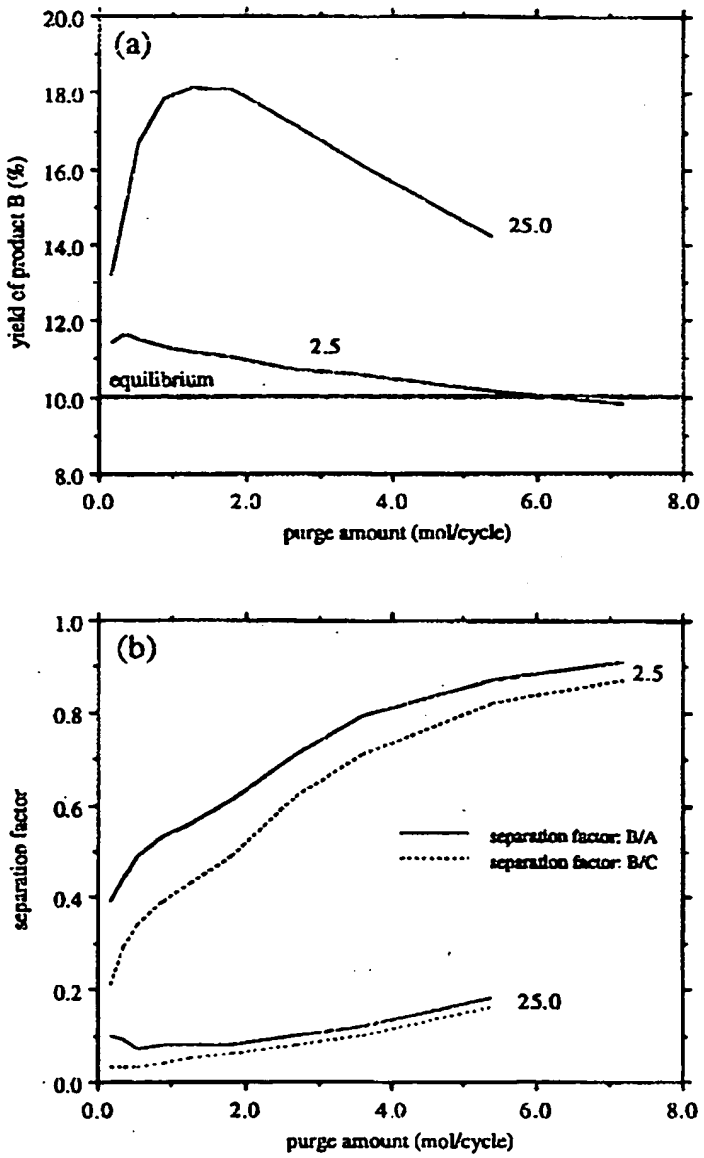

Fig. 4. (a) Total yield of product B and (b) separation factors as a function of the purge amount; parameter = $m_0 \times 10^7$.

In Fig. 5, calculations of Y_B as a function of the combined effects of the purge amount and the cycle time settings are shown. In this case, the different cycle time settings correspond to different feed gas and purge gas flow rates. For example, for a given purge amount, any increase in the duration in the purge step will result in a decrease in the purge gas flow

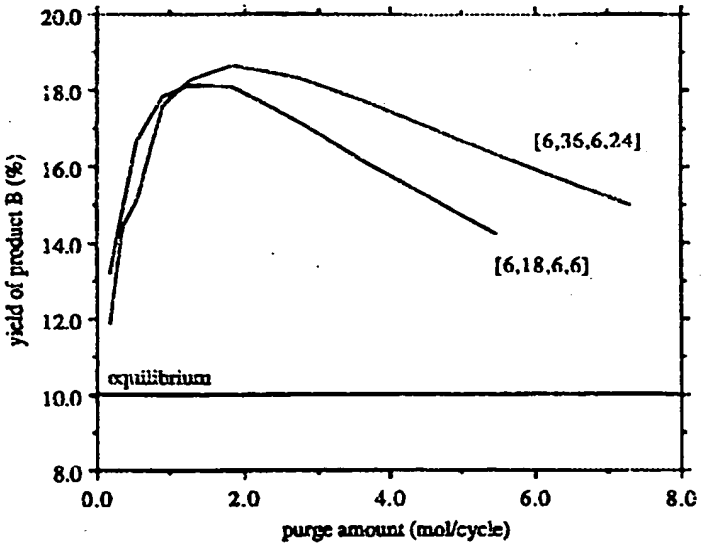

Fig. 5. Total yield of product B as a function of the purge amount; parameter = process step time setting (s) for the pressurisation, product delivery, depressurisation and purge steps, correspondingly.

rate during this step. The results indicate an optimum purge amount, this a function of the product gas flow rate.

The relationship of the separation factor to reaction conversion is further demonstrated by considering the effect of the product amount on Y_B, this again for a purge cycle. In Figs. 6a and 6b Y_B is shown to decrease with increasing product amount, whilst $S_{B/C}$ and $S_{B/A}$ approach unity. This loss in separation performance with increasing product amount is in agreement with conventional PSA operation; see, for example, Kirkby [16] and Espatalier-Noel [17].

5. Discussion

The enhancement of reaction by PSA has been indicated by the above calculations. For a reversible dissociation reaction, separation of the product species along the length of a PSR bed leads to a reduction in the backward reaction rate (e.g. $B + C \rightarrow 2A$), and subsequently enhancement of the net reaction in the forward direction. The inclusion of a purge step is shown to be particularly beneficial in enhancing this separation, and hence reaction. Whilst component separation factors provide a useful indication of the degree of reaction enhancement, the complex relationships between the gas residence time and the degree of separation and reaction precludes any quantitative relationship. This was demonstrated in Figs. 4a and 4b in which optimum conditions could not be correlated to the separation factor data.

In addition to the spatial separation of the reaction species, a second possible mechanism responsible for reaction enhancement can be attributed to the transfer of a product species,

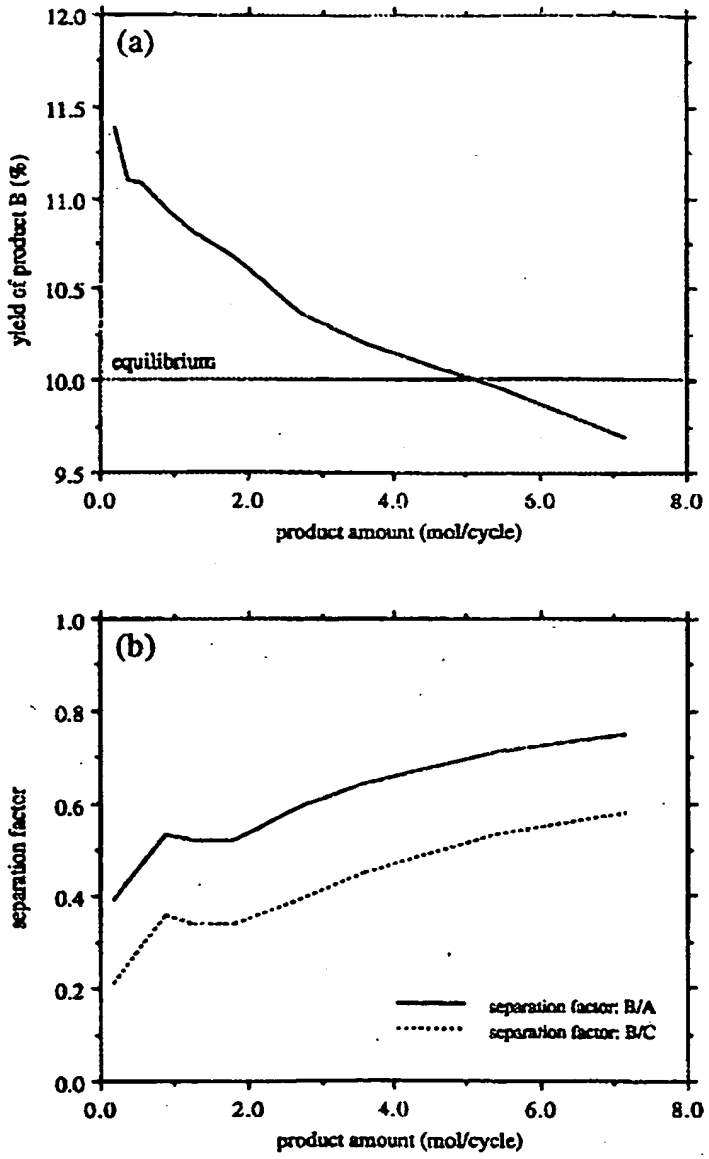

Fig. 6. (a) Total yield of product B and (b) separation factors as a function of the product amount for a purge cycle.

say B, from the gas phase to the adsorbed phase through adsorption. The depletion of B from the gas phase results in further reaction for product formation. During the depressurisation step, the relatively large gas flow rates, and hence short gas residence times for reaction, then allows the collection of desorbed B in the exhaust stream. Preliminary calculations in this work have demonstrated this effect for the single product reaction A ⇌ B,

in which the adsorption of B was again found to give PSR yields greater than that attainable at the reaction equilibrium, i.e., yields of approximately 5% in excess of the equilibrium yield.

As mentioned above, real dehydrogenation reactions are complicated by the effects of pressure on the reaction equilibrium. Operating regions in which a PSR exceeds the best steady state PFR yield (for a given design), or highest equilibrium yield, are currently being sought for such reactions. As experimental verification for the enhancement of catalytic reaction by PSA, a multimodal lab-scale PSR is also being constructed. The dehydrogenation of methylcyclohexane to toluene has been chosen as a test reaction in the first instance. A commercial $Pt-Al_2O_3$ catalyst will be used and admixed with a selective zeolite or silicalite adsorbent. For this real reaction and adsorption system, any effects due to, for example, pressure gradients or mass transfer limitations, will be assessed using the OCFE based model described in Section 2.3.

Finally, theoretical studies will continue to assess the effects of operating conditions and modes of operation on the PSR performance. Explorative calculations for the optimum operating conditions for a purge cycle PSR are also being carried out. Further potential areas of research include pressure swing reaction for enhancing product selectivity, and with the advent of zeolitic catalysts, the use of these combined adsorbents/catalysts in a PSR.

6. Conclusions

Models of a novel reactor which combines separation by PSA and catalytic reaction have been developed, and tested for their numerical precision. For an asymptotic case, in which there is the ideal propagation of concentration wave fronts, and for the reversible dissociation reaction $2A \Leftrightarrow B + C$, almost two-fold improvements over the equilibrium yield of B have been predicted. When compared to conventional steady flow reactors therefore, potential advantages of a PSR include a higher reactor productivity, or a lower temperature of operation for a given conversion. The latter will lead to savings in the energy requirements of the process, and prolong the activity of the catalyst or, indeed, could make a catalytic process feasible in cases where conventional catalytic reactor operation would be impossible. When compared to early examples of adsorptive reactors, e.g. the chromatographic reactors, a PSR offers process simplicity and the continuous delivery of product gas, and is thus suitable for large scale operation. Experimental verification of reaction enhancement by a PSR is currently underway; the more facile dehydrogenation reaction of methylcyclohexane to toluene (at ca. 473K) has been chosen in the first instance, for which a mixture of a selective zeolite adsorbent for toluene and a platinum based reforming catalyst is being employed.

Notation

C gas phase concentration, mol m^{-3}

k_f forward reaction rate constant, $m^6\ kg^{-1}\ mol^{-1}\ s^{-1}$

K_c reaction equilibrium constant
L bed length, m
L_c cell length, m
m adsorption isotherm gradient, mol kg^{-1} Pa^{-1}
P pressure, Pa
P' pressure parameter, s^{-1} (see Eq. (3))
r_x reaction rate, mol kg^{-1} s^{-1}
R gas constant, $=8.314$ J mol^{-1} K^{-1}
S cell state equation for concentration gradient; see Eqs. (12) and (13)
S_{ij} separation factor for components i and j; see Eqs. (15)
t time, s
T temperature, K
u superficial gas velocity, m s^{-1}
x average mole fraction
y gas phase mole fraction
Y total reaction yield; see Eq. (14)
z axial space coordinate, m

Greek

β adsorption parameter (see Eq. (4))
ε total bed voidage
ν power law coefficient
ρ solid density, kg m^{-3}

Subscripts

0, L feed end condition, product end condition
A, B, C, i component identifiers
c cell identifier

References

[1] S.Z. Roginskii, M.I. Yanovskii and G.A. Gaziev, Dokl. Akad. Nauk SSSR, 140 (1961) 1125.
[2] B.M. Magee, Ind. Eng. Chem. Fundam., 2 (1963) 32.
[3] J.M. Loureiro and A.R. Rodrigues, in Adsorption: Science and Technology, Kluwer Academic Publishers, New York, 1989.
[4] K. Takeuchi and Y. Uraguchi, J. Chem. Eng. Jpn., 10 (1977) 455.
[5] T. Petroulas, R. Aris and R.W. Carr, Chem. Eng. Sci., 40 (1985) 2233.
[6] B.B. Fish and R.W. Carr, Chem. Eng. Sci., 41 (1989) 661.
[7] D.M. Ruthven, Principles of Adsorption and Adsorption Processes, John Wiley and Sons, New York, 1984.
[8] R.T. Yang, Gas Separation by Adsorption Processes, Butterworths, Boston, 1987.
[9] P.I. Barton and C.C. Pantelides, AIChE J., (1994) in press.
[10] C.D. Holland and A.I. Liapis, Computer Methods for Solving Dynamic Separation Problems, McGraw-Hill, New York, 1983.
[11] J.E.P. Morgan and N.F. Kirkby, Chem. Eng. Res. Des., (1994) in press.
[12] G.G. Vaporciyan and R.H. Kadlec, AIChE J., 33 (1987) 1334.
[13] E. Alpay, Ph.D. Dissertation, Dept. of Chem. Eng., University of Cambridge, UK (1992).
[14] E. Alpay, C.N. Kenney and D.M. Scott, Chem. Eng. Sci., 48 (1993) 3173.

[15] Z.P. Lu, J.M. Loureiro and A.E. Rodrigues, in A.E. Rodrigues (Editor), Simulation of Pressure Swing Adsorption Reactors, Conf. Proc. for Chempor'93, Porto, Portugal, 1993, pp. 75–82.
[16] N.F. Kirsby, Ph.D. Dissertation, Dept. of Chem. Eng., University of Cambridge, UK (1983).
[17] P.M. Espatalier-Noel, Ph.D Dissertation, Dept. of Chem. and Process Eng., University of Surrey, Guildford, UK (1988).